Mesoscale Convective Complexes and Persistent Elongated Convective Systems over the United States during 1992 and 1993

CHRISTOPHER J. ANDERSON AND RAYMOND W. ARRITT

Department of Agronomy, Iowa State University, Ames, Iowa

(Manuscript received 5 February 1997, in final form 12 June 1997)

ABSTRACT

Large, long-lived convective systems over the United States in 1992 and 1993 have been classified according to physical characteristics observed in satellite imagery as quasi-circular [mesoscale convective complex (MCC)] or elongated [persistent elongated convective system (PECS)] and cataloged. The catalog includes the time of initiation, maximum extent, termination, duration, area of the −52°C cloud shield at the time of maximum extent, significant weather associated with each occurrence, and tracks of the −52°C cloud-shield centroid.

Both MCC and PECS favored nocturnal development and on average lasted about 12 h. In both 1992 and 1993, PECS produced −52°C cloud-shield areas of greater extent and occurred more frequently compared with MCCs. The mean position of initiation for PECS in 1992 and 1993 followed a seasonal shift similar to the climatological seasonal shift for MCC occurrences but was displaced eastward of the mean position of MCC initiation in 1992 and 1993. The spatial distribution of MCC and PECS occurrences contain a period of persistent development near 40°N in July 1992 and July 1993 that contributed to the extreme wetness experienced in the Midwest during these two months.

Both MCC and PECS initiated in environments characterized by deep, synoptic-scale ascent associated with continental-scale baroclinic waves. PECS occurrences initiated more often as vigorous waves exited the intermountain region, whereas MCCs initiated more often within a high-amplitude wave with a trough positioned over the northwestern United States and a ridge positioned over the Great Plains. The low-level jet transported moisture into the region of initiation for both MCC and PECS occurrences. The areal extent of convective initiation was limited by the orientation of low-level features for MCC occurrences.

1. Introduction

Mesoscale convective complexes (MCC; Maddox 1980) are large, long-lived convective systems that exhibit a quasi-circular cloud shield (infrared temperature ≤ -52°C) in infrared (IR) satellite imagery. Table 1 lists the specific criteria that must be met in order to classify a convective system as an MCC. These criteria differ slightly from the origional criteria established by Maddox (1980) in order to simplify the documentation procedure (Augustine and Howard 1988). Research has shown that MCCs can induce adjustments by the large-scale atmospheric circulation (e.g., Fritsch and Maddox 1981; Menard and Fritsch 1989) and can produce hazardous weather over a large region. Thus, MCCs represent a challenging and important forecast problem.

Annual summaries of MCC occurrences over the United States (Maddox 1980; Maddox et al. 1982; Rodgers et al. 1983; Rodgers et al. 1985; Augustine and Howard 1988; Augustine and Howard 1991) have provided a climatological reference for MCC occurrences. These summaries indicate that on average, about 35 MCC occurrences have affected the United States annually, with a maximum of 59 in 1985 (Augustine and Howard 1988) and a minimum of 23 in 1981 (Maddox et al. 1982). Typically, the southern Great Plains experiences most of the MCC activity during the spring, while the MCC activity shifts northward during the summer. During the fall, the bulk of the MCC activity returns to the southern Great Plains. The distribution of MCC occurrences during a dry hydrological anomaly in the central United States in 1983 did not follow the climatological trends. Rather, a persistent anticyclone over the central United States hindered the moisture flux into the Great Plains that aids the development of MCCs. This resulted in an increased frequency of smaller quasi-circular convective system occurrences north of the Great Plains throughout the summer and fall (Fritsch et al. 1986).

These summaries have also contributed knowledge of large-scale features that support MCC development. Augustine and Howard (1988) used monthly mean **Q**-vector divergence (Hoskins et al. 1978) to compare the synoptic-scale vertical motion for an inactive warm season (1984) with a very active warm season (1985). Their

Corresponding author address: Christopher J. Anderson, Department of Agronomy, 3010 Agronomy Building, Iowa State University, Ames, IA 50011.
E-mail: candersn@iastate.edu

TABLE 1. Modified MCC definition.

Size	Continuous cold-cloud shield (IR temperature $\leq -52°C$) must have an area $\geq 50\ 000$ km^2
Initiation	Size definition is first satisfied
Duration	Size definition must be met for a period of ≥ 6 h
Maximum extent	Continuous cloud shield (IR temperature $\leq -52°C$) reaches maximum size
Shape	Minor axis/major axis ≥ 0.7 at time of maximum extent
Termination	Size definition is no longer satisfied

results showed stronger synoptic-scale ascent at 600 and 400 mb for June 1985 (the month with the largest difference in MCC occurrences between 1984 and 1985) suggesting that this period of persistent MCC development was supported by a persistent, upper-level mass–momentum imbalance in the synoptic-scale circulation. Augustine and Howard (1991) addressed low-level features supporting MCC development by compositing 850-mb wind, mixing ratio, geopotential height, and 500-mb geopotential height for weeks of frequent MCC occurrences and weeks of infrequent MCC occurrences in 1986 and 1987. The active weeks were dominated by a deep tropospheric ridge centered over the southeastern United States with low-level moisture flux into the central plains region. Most MCC occurrences were observed near the intersection of a low-level jet (LLJ) and a zonally oriented low-level front. The inactive periods were dominated by a 500-mb trough over the southeastern United States and low-level moisture transport into that region.

Unfortunately, large, long-lived non-MCC convective system occurrences have not been documented as thoroughly despite a potential for hazardous weather similar to that of MCC occurrences. Only one of the annual MCC summaries (Maddox et al. 1982) has included a list of ''non-MCC significant mesoscale convective events.'' The list does not allow for a comparison with the MCC events because satellite characteristics and a description of the life cycle of each event were not included. Bartels et al. (1984) performed a satellite-based climatology for 1978–83 over the Stormscale Operational and Research Meteorology (STORM)-Central project domain that included convective systems exceeding 250 km along their major axis and 3 h during their life cycle. MCC occurrences and large, long-lived linear convective system occurrences fit within these criteria. In their tabulation, large, long-lived linear convective systems (their ''large cloud lines'') totaled about one-third of the number of MCC occurrences.

We address the lack of information concerning large, long-lived non-MCC mesoscale convective system occurrences using a comparative study with MCC occurrences in 1992 and 1993. We refer to a large, long-lived non-MCC mesoscale convective system as a ''persistent elongated convective system'' (PECS). Formally, we define a PECS as a mesoscale convective system that fulfills the size and duration criteria, *but not the shape criterion*, of the MCC definition. That is, a PECS must meet every criterion in Table 1 except the ratio of the minor to major axis does not exceed 0.7. While the internal circulation of convective systems is not addressed with a satellite-based definition (as pointed out by Maddox 1980), observational studies (e.g., Fritsch and Maddox 1981), as well as the duration and size of these convective systems, suggest that most contain a distinct, mesoscale circulation. In order to diminish the likelihood that extremely long lines of convective elements (convective systems not likely to contain a distinct, mesoscale circulation) meet our PECS criteria, we established a lower limit of 0.2 for the ratio of the minor to major axis. Our comparative study consists of a tabulation of PECS and MCC occurrences in 1992 and 1993 and composites of environmental features near the time of initiation. The tabulation of MCC occurrences for 1993 has added to the climatological reference base an account of MCC occurrences during an extreme wet hydrological anomaly in the Great Plains [for an overview of the 1993 flood see e.g., Kunkel et al. (1994)].

2. Data and methodology

a. Data sources

Cloud-top characteristics in *GOES-7* IR digital satellite imagery for 1992 and 1993 were analyzed with a version of the automated routine developed by Augustine (1985). The routine searches all pixels within the image that represent cloud-top temperature less than or equal to $-52°C$ and uses a harmonic analysis technique to compute the best-fit ellipse for the $-52°C$ cloud-shield perimeter. The $-52°C$ cloud-shield centroid and eccentricity are computed from the best-fit ellipse. We also view imagery for each system to check that the automated procedure does not detect spurious systems. We then tabulate the duration of the MCC or PECS occurrence, size of the $-52°C$ cloud shield at maximum extent, and hourly position of the $-52°C$ cloud-shield centroid. In addition, we have summarized significant weather associated with each MCC and PECS occurrence from the National Oceanic and Atmospheric Administration/National Environmental Satellite, Data, and Information System (NOAA/NESDIS) publication *Storm Data.*

Archived data from the National Meteorological Center (NMC) Global Data Analysis System (GDAS; Kalnay et al. 1990) were used to construct composite analyses near the times of MCC and PECS initiation. In both 1992 and 1993, the GDAS used the T80 resolution (equivalant to about 200-km grid spacing) Medium Range Forecast Model to provide the background or ''first-guess'' fields for the analyses. Over data-rich areas such as North America, the GDAS analyses mainly reflect the observations with relatively little influence from the model-based first-guess fields. This dataset

contains 2.5° latitude–longitude grids at 0000 and 1200 UTC of surface temperature, geopotential height, and wind at 1000, 850, 700, 500, 400, 300, 250, 200, 150, 100, 70, and 50 mb. Relative humidity is also included at levels from 1000 through 300 mb.

b. Fixed-point compositing methods

Composites of atmospheric parameters for June–July 1993 were constructed by averaging data from 0000 UTC GDAS grids at each grid point over every day in June and July. Data were taken solely from 0000 UTC grids in order to limit the influence of the diurnal evolution of the atmospheric circulation and the influence of large convective systems. A deviation from the background composite on days when MCC or PECS occurrences initiated between 1800 and 0600 UTC (within 6 h of 0000 UTC) in June–July 1993 was computed by differencing grids on these days from the background composite grids. The deviations were then averaged over the number of MCC or PECS occurrences to produce MCC and PECS deviation composites.

Augustine and Howard (1991) described this as a ''fixed point'' compositing technique and pointed out that this technique retains persistent large-scale features while smoothing out recurrent mesoscale features. This compositing technique allows for comparisons between the large-scale circulation associated with the initiation of MCC and PECS occurrences in June–July 1993 with the well-documented large-scale circulation of June–July 1993.

c. Storm-relative compositing methods

A new storm-relative compositing technique was developed in an attempt to reduce spatial distortion and noise in the composite fields. Data from the 2.5° GDAS grids were repositioned within a 5000 km × 3000 km stereographic grid centered on each convective system's centroid. (Grid spacing of the stereographic grid was 100 km.) We used 0000 UTC grids for convective systems that initiated between 2200 and 0400 UTC and 1200 UTC grids for convective systems that initiated between 1000 and 1600 UTC. These time ranges are designed so that our composites reflect environmental conditions prior to initiation for a majority of the occurrences in our tabulation. The deviations of the data values from the center gridpoint value were composited, and separate composites were also constructed from the raw values for each occurrence of a convective system. Compositing the deviation values reduces the ambiguity that arises from seasonal trends in the mean value of the atmospheric parameter being composited, better fulfilling the assumption of the composite-before-objective analysis technique that the phenomenon and its environment are similar from event to event. Therefore, these composites retain environmental spatial variability while introducing less spatial noise than composites of the raw values. A variant of the Barnes (1994) objective analysis routine was applied to the composited data [following the approach suggested by Achtemeier (1989)] in order to map the composited data onto the stereographic grid. The response function for our implementation of the Barnes scheme is shown in Fig. 1. Once the data were mapped onto the stereographic grid, the mean of the raw center gridpoint value was added to the composited deviation values in order to produce fields of meteorologically relevant magnitudes. Derived terms, like advection, vorticity, and **Q**-vector divergence, were computed after the meterological fields were recreated from the deviations.

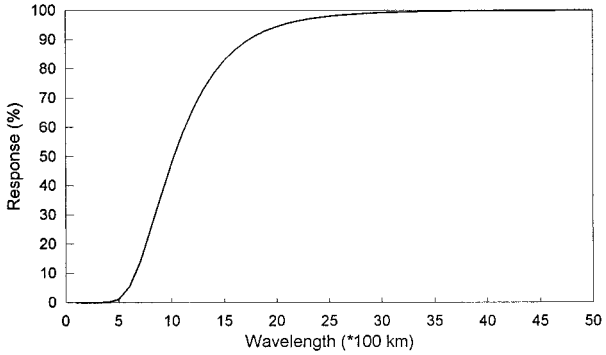

FIG. 1. Response function of the Barnes analysis routine applied to the composite storm-relative data.

A stereographic grid was used rather than a latitude–longitude grid in order to minimize spatial distortion in the composite. This distortion arises from the variation with latitude of the absolute distance for a constant longitudinal separation and has been recognized as a source of error by Maddox (1983). The map factor for a stereographic grid varies less with latitude than does the map factor for a latitude–longitude grid, reducing the spatial distortion.

MCC-relative and PECS-relative composites were generated by applying this technique to 38 MCC occurrences and 70 PECS occurrences from our tabulation. The composites do not contain all convective-system occurrences, because the archived GDAS analyses did not contain data on 15 July, 3 August, 20 September, and 7 October in 1992 and 30 March, 1 May, and 8 July in 1993.

3. Catalog of MCC and PECS in 1992 and 1993

a. MCC and PECS occurrences in 1992

In 1992, a total of 27 MCC and 77 PECS occurrences were observed over the United States from early March through mid-November. The higher frequency of PECS contrasts with Bartels et al. (1984) who found fewer large cloud-line occurrences than MCC occurrences in 1978–83. The number of MCC occurrences in 1992 was eight less than the annual average. Summaries of MCC and PECS occurrences that include the duration, max-

TABLE 2. MCC occurrences in 1992: T—tornadoes; W—high wind; L—lightning damage; R—heavy rain; F—flash flooding; nK—(number of people) killed; nI—(number of people) injured.

Case number	Date(s)	Initiation (Date/UTC)	Maximum	Termination	Duration (h)	Max. extent (km^2)	Significant Wx
1	12 Apr	12/0200	12/0400	12/1000	8	79 788	No report
2	12 Apr	12/0600	12/1100	12/1400	8	145 076	H, W, F
3	16 Apr	16/0000	16/0200	16/0600	6	196 016	H, F, W
4	16 Apr	16/0100	16/0700	16/1100	10	245 191	No report
5	13–14 May	13/2100	13/0900	14/1700	20	338 200	H, W, L
6	14–15 May	14/2300	14/0700	15/1000	11	100 407	L
7	15–16 May	15/2100	15/2200	16/0400	7	68 382	W, T, H
8	15–16 May	15/2200	15/0400	16/0600	8	72 434	H, W
9	5 Jun	5/0200	5/0600	5/1400	12	111 898	H, T, F, W
10	5–6 Jun	5/2200	5/0800	6/1600	18	300 891	H, T, W, F, L
11	5 Jun	5/0500	5/0800	5/1300	8	94 417	H, T, W, F
12	20 Jun	20/0200	20/0500	20/0900	7	144 672	W, H, L
13	6 Jul	6/0600	6/0800	6/1400	8	104 717	H
14	7 Jul	7/0600	7/1500	7/1900	13	231 685	W, F, L
15	16 Jul	16/1000	16/1000	16/1500	5	147 983	H, W, F
16	22 Jul	22/0200	22/0600	22/1000	8	85 669	F
17	25–26 Jul	25/2300	26/0500	26/0800	9	202 248	W, H, F
18	30 Jul	30/0100	30/0600	30/0900	8	154 460	W, H, T, F
19	3 Aug	3/1300	3/1300	3/2300	10	107 053	W, H
20	4 Aug	4/0500	4/1000	4/1400	9	123 357	W, H
21	5 Aug	5/0100	5/1200	5/1500	14	111 616	H, W, F, L, 9I
22	6 Aug	6/0100	6/0200	6/0700	6	75 019	No report
23	9–10 Aug	9/1800	9/2000	10/0000	6	102 327	H, W, F
24	17–18 Aug	17/2300	18/0700	18/1100	12	149 491	W, H
25	3 Sep	3/0200	3/0900	3/1700	15	192 253	W, H
26	8 Oct	8/1600	8/2000	8/2300	7	98 580	No report
27	3–4 Nov	3/2300	4/0600	4/0600	7	133 802	T, W, H

imum areal coverage of the −52°C cloud shield, and associated significant weather are provided in Table 2 and Table 3, respectively.

In general, PECSs in 1992 generated a larger −52°C cloud shield and persisted longer than MCCs (Table 4). Despite this, MCC occurrences typically traveled a greater distance based on the centroid positions at initiation, maximization, and termination. (We recognize that the centroids for the PECS occurrences do not take into account the orientation of the PECS occurrences. As a result, it is impossible to determine the entire region affected by an individual PECS occurrence. However, because the centroid is the median latitude and longitude of the −52°C cloud-top area, centroid tracks retain an average motion for the PECS and MCC occurrences.) The westward (i.e., positive) skewness in the distribution of MCC occurrences and the eastward skewness in the distribution of PECS occurrences suggest that most of the PECS occurrences initiated, maximized, and terminated farther east of the MCC occurrences than indicated by the mean positions.

Both MCC and PECS frequently initiated in the late afternoon and developed overnight (Fig. 2). PECS displayed greater variability in the time of initiation with a higher percentage of occurrences initiating between 0600 and 2000 UTC. We also found that the percentage of MCCs that initiated in the evening hours increased during the summer months. (Local sunset in the central United States is around 0000 UTC at the equinoxes and 0200–0300 UTC at the summer solstice.) Notice in Fig. 3a that the peak frequency of MCC occurrence was observed in July. These findings are in agreement with previous MCC summaries that reported the highest frequency of MCC occurrences during summer nights (e.g., see Augustine and Howard 1991). The summertime peak was not as pronounced for the PECS occurrences, which also had a secondary maximum in September (Fig. 3b).

Most of the early-season MCCs were observed over the southern portion of the United States. The mean position of MCC occurrence then shifted northward during June (Fig. 4). These characteristics of the distribution are consistent with the climatological distribution of MCC occurrences. However, few MCCs were observed north of 40°N in July 1992, so that the northward shift of the 1992 mean position of MCC initiation was much less than the climatological mean seasonal shift in position of MCC occurrence. The mean position of PECS occurrence (Fig. 5) shifted farther northward during June and July 1992 than did the mean position of MCC occurrences and returned to the southern United States in mid-September. Similar to the distribution of MCC occurrences, a period of persistent PECS occurrences was observed near 40°N in June.

b. MCC and PECS occurrences in 1993

From late March through mid-September of 1993, a total of 28 MCCs and 44 PECSs were observed over

TABLE 3. As in Table 2 except for PECS occurrences in 1992. Asterisk denotes missing data.

Case number	Date(s)	Initiation (Date/UTC)	Maximum	Termination	Duration (h)	Max. extent (km^2)	Significant Wx
1	4 Mar	4/0100	4/0600	*	*	258 434	T, H, W, F, L
2	6 Mar	6/1000	6/1200	6/2000	10	103 373	No report
3	9–10 Mar	9/1900	10/1700	11/0900	38	393 938	H, W, T
4	18 Mar	18/0300	18/1300	18/2200	19	175 519	H, W
5	6 Apr	6/0400	6/1000	6/1300	9	138 951	No report
6	10 Apr	10/0500	10/0800	10/1800	13	105 163	H. W
7	11 Apr	11/0000	11/0600	11/1300	13	572 739	H, W, F, L, T
8	13 Apr	13/0700	13/1200	13/1800	11	94 992	No report
9	17 Apr	17/0000	17/0600	17/1000	10	304 639	H, W, F, T
10	18 Apr	18/0400	18/0900	18/1600	12	306 917	F, W
11	19 Apr	19/0800	19/0800	19/1400	6	98 269	W, H, L
12	25 Apr	25/0300	25/1100	25/1600	13	290 023	W, H, F, L
13	2–3 May	2/1500	3/0100	3/0500	14	157 883	W
14	16 May	16/0600	16/0700	16/1400	8	295 670	T, H, W
15	16–17 May	16/2100	17/0000	17/0400	7	163 153	F, T, W, H
16	22–23 May	22/2000	22/2300	23/1600	20	265 485	F, H, T, W
17	31 May	31/0800	31/1000	31/1600	8	104 385	No report
18	1 Jun	1/0500	7/0700	1/1100	6	82 902	No report
19	7 Jun	7/0000	7/0200	7/0600	6	107 593	L
20	9 Jun	9/0300	9/0600	9/0900	6	94 045	H, W, T, F
21	13–14 Jun	13/2100	14/0300	14/1300	16	209 053	H, L
22	14–15 Jun	14/1000	14/1400	15/0600	20	125 178	H, F, W
23	15–16 Jun	15/2300	16/0500	16/1500	16	340 871	H, T, L, W, F
24	16–17 Jun	16/2300	17/0500	17/1400	15	242 395	H, T, W
25	17–18 Jun	17/2000	17/2300	18/1200	16	133 400	W, H, L, T, F
26	19–20 Jun	19/1700	20/000	20/0400	11	126 079	H, W, T, F, L
27	19–20 Jun	19/2300	20/0200	20/0600	7	142 431	H, W, T, F, L
28	21 Jun	21/0300	21/0300	21/0800	5	129 403	No report
29	1 Jul	1/0000	1/0400	1/1100	11	235 181	H, W, T
30	2 Jul	2/0400	2/1300	2/1700	13	164 798	H, W, L, F, T
31	3–4 Jul	3/1800	3/2200	4/0100	7	128 445	H
32	3–4 Jul	3/2000	4/0000	4/0200	6	98 638	T, L, W, H, F
33	4–5 Jul	4/2100	5/0400	5/1300	16	347 244	H, L, T, W
34	5 Jul	5/0400	5/0900	5/1800	14	131 859	L, W, H
35	8 Jul	8/0300	8/0800	8/1900	16	321 994	H, W, L
36	9 Jul	9/0100	9/0600	9/0900	8	75 957	H
37	11 Jul	11/0100	11/0300	11/0700	6	115 479	H
38	15–16 Jul	15/1800	15/1900	16/0100	7	111 949	T
39	16 Jul	16/0100	16/0400	16/0800	7	179 230	T, W, H, F, L
40	18 Jul	18/0200	18/0600	18/0900	7	103 576	F, H
41	19 Jul	19/0000	19/0500	19/0700	7	97 381	H, W, T
42	24–25 Jul	24/2300	25/0200	25/1100	12	105 707	T, F, L
43	26–27 Jul	26/2200	27/0300	27/0600	8	169 826	H, L, W
44	26–27 Jul	26/2200	27/0600	27/0600	8	190 076	L, F, W
45	30–31 Jul	30/2300	31/0200	31/0800	9	104 352	H, F, W, L
46	7 Aug	7/0000	7/0600	7/1400	14	326 962	H, W, L
47	8 Aug	8/1200	8/1600	8/1900	7	98 583	F, L
48	10 Aug	10/0200	10/0800	10/1300	11	175 736	T
49	10–11 Aug	10/2200	11/0700	11/1200	14	286 851	H, W, F
50	11–12 Aug	11/2300	12/000	12/0800	9	103 750	L, F, H, W
51	2 Sep	2/0000	2/0400	2/0900	9	83 057	No report
52	5 Sep	5/0500	5/0900	5/1200	7	194 880	No report
53	5 Sep	5/1100	5/1100	5/1800	7	118 575	W, H
54	6 Sep	6/0200	6/0500	6/1200	10	280 833	T, H, F, W
55	7 Sep	7/0300	7/0600	7/1100	8	131 929	H, L
56	7 Sep	7/0300	7/0900	7/1800	15	152 010	T, H, L
57	8 Sep	8/0300	8/0500	8/0900	6	250 321	W, L
58	8–9 Sep	8/1800	9/0100	9/0500	11	79 773	F, H
59	9–10 Sep	9/0900	10/0300	10/0900	24	423 077	H, W, L, F
60	10–11 Sep	10/1100	11/0100	11/1100	24	209 775	H, W, L, F
61	14 Sep	14/0600	14/1200	14/1900	13	388 828	F
62	15 Sep	15/0200	15/0600	15/1500	13	132 215	F
63	16 Sep	16/0100	16/1100	16/1700	16	258 180	H, W, F, L
64	17 Sep	17/0600	17/1000	17/1200	7	110 346	W
65	18 Sep	18/0200	18/0900	18/1500	13	195 840	H, W
66	19 Sep	19/0900	19/1400	19/1800	9	148 982	No report
67	20 Sep	20/0200	20/0400	20/1000	8	112 068	W, H, L

TABLE 3. (*Continued*)

Case number	Date(s)	Initiation (Date/UTC)	Maximum	Termination	Duration (h)	Max. extent (km^2)	Significant Wx
68	7 Oct	7/0500	7/0900	7/1100	6	158 516	R, F
69	9 Oct	9/0200	9/0800	9/1300	11	144 491	W, H, L
70	9 Oct	9/0200	9/1000	9/1200	10	159 159	R
71	30 Oct	30/0000	30/0500	30/1300	13	237 027	H, W
72	1 Nov	1/0500	1/0700	1/1300	8	194 383	W, H, T, L
73	1–2 Nov	1/1100	2/0200	2/0500	18	153 558	W, T, H
74	2–3 Nov	2/0400	2/1300	3/1300	33	270 372	W
75	11 Nov	11/0600	11/1200	11/1500	9	76 414	No report
76	12–13 Nov	12/0800	13/0400	13/1500	31	297 526	F, W
77	20–22 Nov	20/2100	21/0600	22/1200	39	348 530	T, W, H, F, 26 K, 500+ I

the United States. Similar to 1992, MCC occurrences were less frequent than the annual average (by seven), and PECSs were more frequent than MCCs. Tables 5 and 6 provide summaries for MCC and PECS occurrences, respectively, that include the duration, maximum areal coverage of the −52°C cloud shield, and associated significant weather.

The mean PECS occurrence was larger than the mean MCC, while MCCs in general were longer lived and traversed a greater distance than PECSs (Table 4). PECS occurrences initiated, maximized, and terminated farther east and south than MCCs. Both MCCs and PECS favored nocturnal development (Fig. 2). The peak frequency of occurrence was observed in July (Fig. 3a). In addition, a larger percentage of MCCs in the summer months initiated in the late afternoon than those in the spring months. The month of peak frequency for PECS occurrences was June. Unlike the MCC occurrences, the percentage of PECS occurrences initiating in the evening did not change much between spring and summer. PECSs were more frequent during the spring and fall than MCCs.

Similar to 1992, PECS occurrences in 1993 (Fig. 7) followed a more pronounced seasonal migration of the mean position than did the MCCs (Fig. 6). Both distributions showed a concentration of systems near 40°N. This

TABLE 4. Selected MCC and PECS occurrence statistics [skewness] {kurtosis}.

	1992		1993	
	MCC	PECS	MCC	PECS
Number of occurrences	27	77	28	44
Maximum extent of −52°C cloud shield (km^2)	145 098 [1.259] {0.939}	188 009 [1.290] {1.665}	184 285 [1.171] {1.522}	193 167 [0.705] {−0.337}
Duration (h)	9.6 [1.273] {1.015}	12.2 [2.047] {4.584}	13.9 [1.859] {3.729}	12.4 [1.056] {0.981}
Initiation position (north lat, west long)	38.81, 100.47 [0.221, 0.442] {−0.393, −0.146}	39.09, 95.17 [−0.053, −0.292] {−1.010, 0.096}	40.80, 100.76 [−0.938, −0.064] {0.373, −0.137}	38.73, 97.01 [0.070, −0.606] {−0.600, 0.180}
Maximum position (north lat, west long)	38.28, 98.15 [0.164, 0.494] {−0.100, −0.314}	38.94, 93.39 [−0.179, −0.418] {−0.960, 0.083}	40.84, 96.94 [−0.754, 0.458] {−0.085, −0.210}	38.83, 94.52 [0.009, −0.279] {−0.377, 0.259}
Termination position (north lat, west long)	37.96, 95.61 [−0.018, 0.258] {−0.409, −0.081}	39.37, 90.44 [−0.004, −0.482] {−0.768, 0.218}	40.04, 93.19 [−0.918, −0.336] {0.545, 1.100}	38.61, 90.89 [−0.051, −0.195] {0.347, 0.240}
	All MCC		All PECS	
Initiation position (north lat, west long)	39.83, 100.62 [−0.335, 0.249] {−0.460, −0.056}		38.95, 95.84 [−0.008, −0.414] {−1.158, −0.444}	
Maximum position (north lat, west long)	39.59, 97.53 [−0.287, 0.593] {−0.460, 0.076}		38.90, 93.80 [−0.124, −0.447] {−0.823, −1.375}	
Termination position (north lat, west long)	39.20, 94.38 [−0.444, 0.043] {−0.265, 0.624}		39.09, 90.60 [0.029, −0.482] {−0.794, −1.136}	

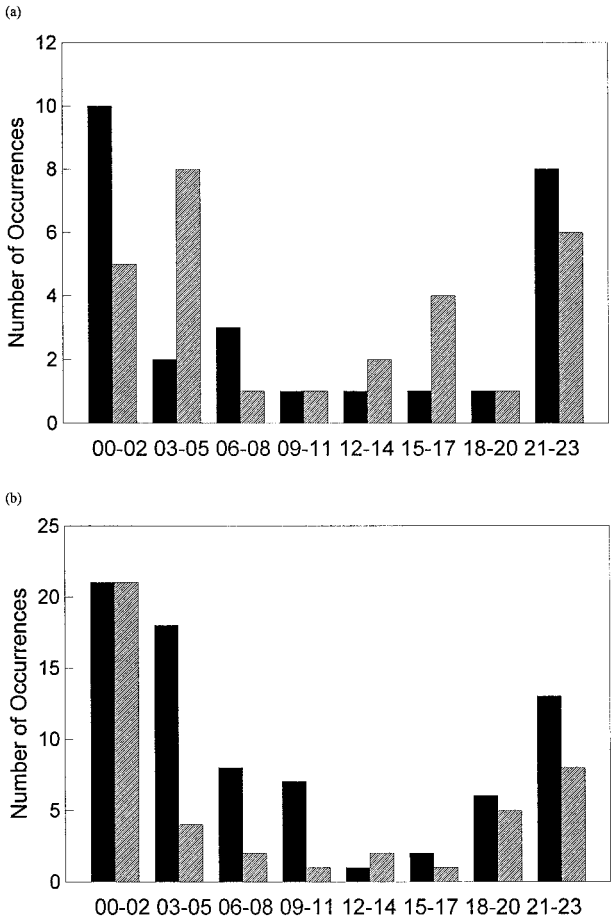

FIG. 2. Hourly distribution of the time of initiation (UTC) for (a) MCC and (b) PECS occurrences in 1992 (solid) and 1993 (hatched).

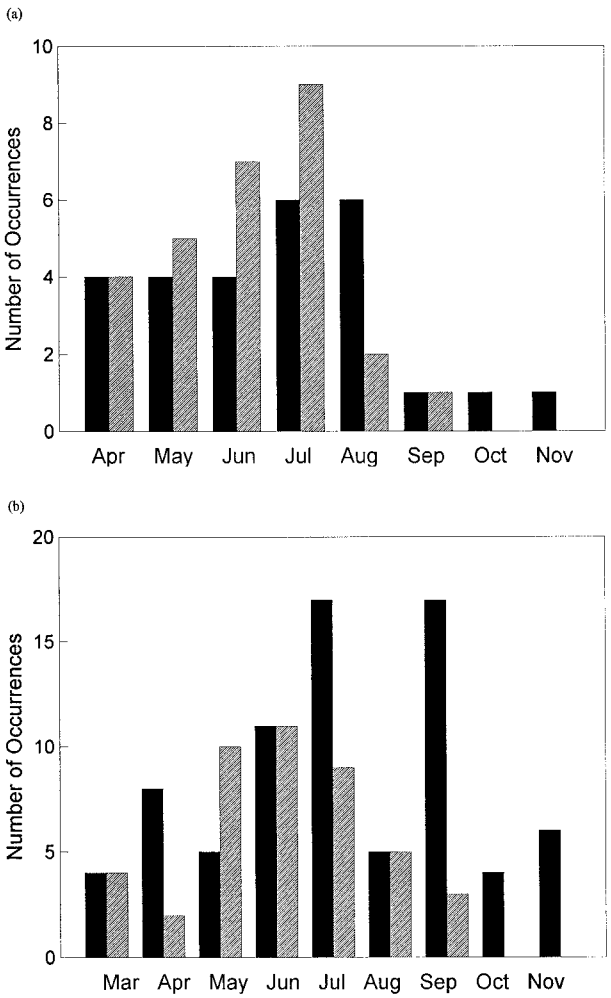

FIG. 3. Monthly distribution of (a) MCC and (b) PECS occurrences for 1992 (solid) and 1993 (hatched).

spatial concentration of MCC occurrences (reflected in Table 4 as positive kurtosis) was more pronounced, extending through much of the summer, whereas the persistence of PECS occurrences spanned the first half of June.

c. General comparison of MCC and PECS occurrences

Bartels et al. (1984) found that large cloud lines and MCCs in their climatology displayed similar diurnal characteristics. Our results support their finding as both types of systems favored initiation in the late afternoon (Fig. 2) and developed overnight, typically lasting about 12 h (Table 4). Bartels et al. (1984) reported that the occurrence of large cloud lines increased during the summer, similar to our findings, but their summertime peak was not as pronounced as the peak in our tabulation. In addition, our combined tabulation for 1992 and 1993 reveals a second peak in the frequency of PECS occurrence in September (Fig. 3). Their study was limited to convective system occurrences prior to August over the STORM-Central domain.

PECS occurrences initiated and developed farther east than MCC occurrences. The mean centroid positions do not fully describe this difference as the distribution of PECS occurrences contains a bias eastward of the mean centroid positions. In fact, most MCC occurrences terminated prior to 95°W (about the mean initiation position of PECS occurrences) as evidenced in the distribution of MCC occurrences by the westward skewness and clustering about the mean longitude of termination (Table 4).

MCC and PECS occurrences in 1993 on average lasted longer and were larger than in 1992 (Table 4). Cotton et al. (1989) described the MCC as an inertially stable convective system, or a system whose spatial scale is comparable to, or exceeds, the Rossby radius of deformation causing the system to approach geostrophic balance. This description is supported by numerical simulation (Zhang and Fritsch 1987) and observational evidence (Menard and Fritsch 1989). The correlation between size and duration of MCC occurrences found in this and other studies (e.g., Laing and Fritsch 1997) agrees with this description, because the likelihood that the spatial scale of the MCC

FIG. 4. Tracks of −52°C cloud-shield centroids for MCC occurrences in 1992 during (a) March, April, May; (b) June, July, August; and (c) September, October, November.

exceeds the Rossby radius of deformation increases with the size of the MCC (all else being equal). The correspondence between the mean PECS size and duration in our tabulation suggests the possibility that inertially stable vortices may play a role in the persistence of PECS occurrences as well as MCCs. However, the mean MCC occurrence in 1993 persisted longer than the larger mean PECS occurrences in 1992 and 1993, suggesting that this mechanism may not be as effective for PECSs as for MCCs. Further study of the internal circulations within MCCs and PECSs would be needed to address this issue.

d. Contribution to extreme wet periods in 1992 and 1993

Kunkel et al. (1994) cited soil wetness approaching saturation over much of the Midwest beginning in July 1992 as one of seven hydrometeorological factors that contributed to the regional flooding observed in the Midwest during the summer of 1993. Our tabulation contains an extraordinary number of PECS occurrences in June–July 1992 that nearly equaled the total number of large cloud lines in June 1979–83 (13 compared with 14) and surpassed the total number of large cloud lines in July 1978–83 [16 compared with 12; Bartels et al. (1984)]. Most of the PECSs in late June–July 1992 tracked over the eastern portions of the Great Plains and aided soil saturation by contributing heavy rainfall amounts and by reducing evapotranspiration through increased cloud coverage. The anomolous late-season occurrence of large convective systems in 1992 helped to maintain near-saturation soil wetness through the fall of 1992 into the spring of 1993.

Another factor contributing to the 1993 Midwest flood

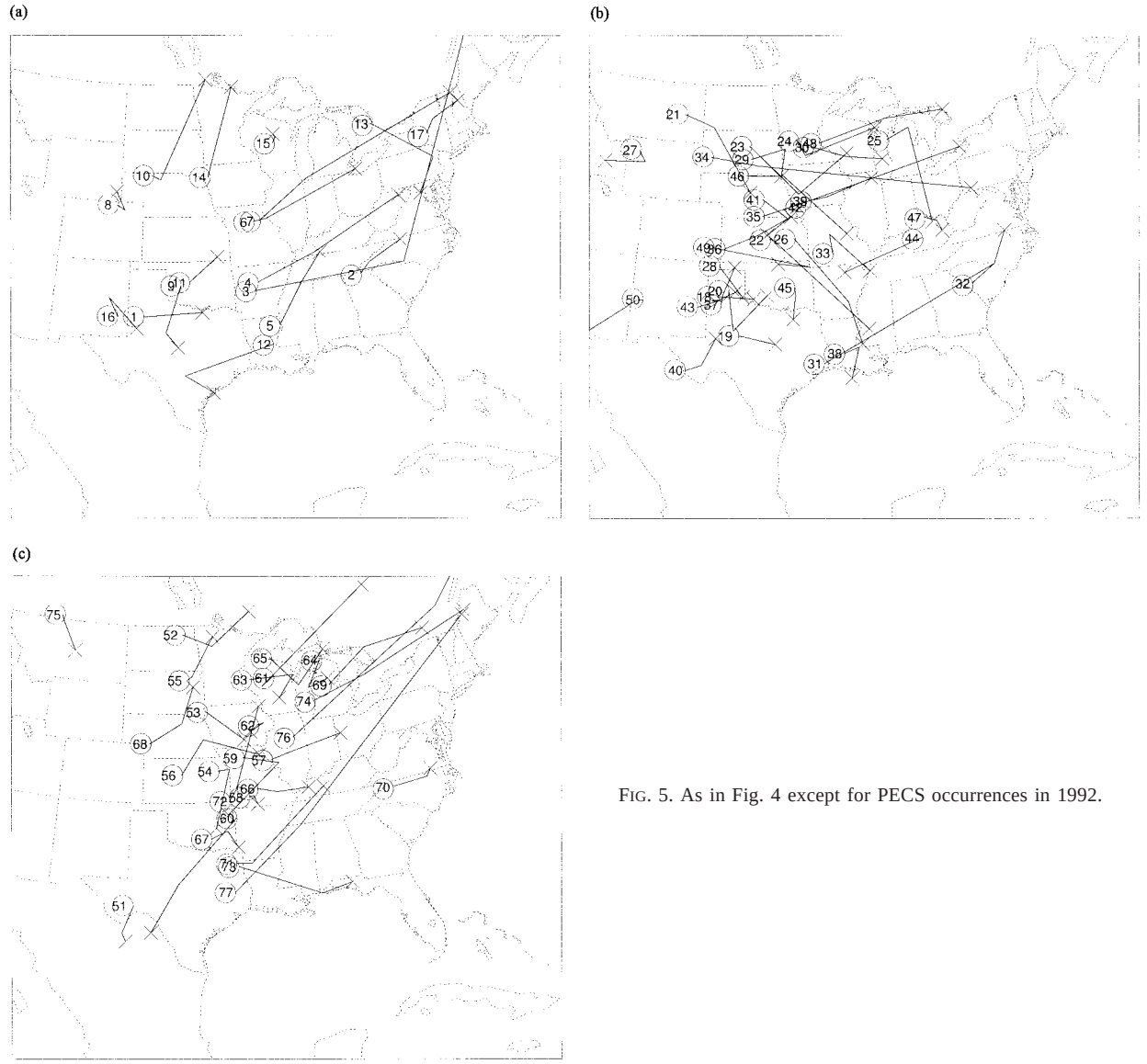

FIG. 5. As in Fig. 4 except for PECS occurrences in 1992.

discussed in Kunkel et al. (1994) is the frequent occurrence of large-sized areas of moderate to heavy rain. They subjectively determined that 70 large-sized areas of moderate to heavy rain affected the Midwest in the summer of 1993 and commented that ''many of the large rain areas were of appropriate scale and shape to suggest the presence of MCCs and MCSs.'' Our tabulation reports 43 MCC and PECS occurrences over the Midwest during the summer of 1993 supporting their characterization of the large-sized rain areas. (This suggests that perhaps surface rainfall observations could be used to infer a more comprehensive climatology of large long-lived convective system occurrences prior to 1978.)

As stated in the introduction, spatial persistence was demonstrated in the distribution of MCC occurrences in 1983, a drought year (Rodgers et al. 1985). In a comparison of quasi-circular convective systems from 1982 and 1983, Fritsch et al. (1986) concluded that storm precipitation frequency and the anomalous persistence of occurrences north of the Midwest contributed more to the drought conditions over the Midwest in 1983 than frequency of occurrence. This notion has some additional support, as regional flooding was not observed in 1985. In that year, more MCC occurrences (59) were observed than in any other year for which the MCC climatologies have been performed; however, the MCCs were less concentrated spatially than in 1983 and 1993 (Augustine and Howard 1988). If considering only the MCC occurrences for 1993, our results would also imply that concentrated occurrences and storm precipitation efficiency were more important factors contributing to regional flooding than frequency, because MCC occur-

TABLE 5. As in Table 2 except for MCC occurrences in 1993.

Case number	Date(s)	Initiation (Date/UTC)	Maximum	Termination	Duration (h)	Max. extent (km^2)	Significant Wx
1	7–9 Apr	7/0900	8/0200	9/0400	43	473 895	H, T, F, W, L
2	12–13 Apr	12/2000	12/2200	13/0200	6	69 718	H, L, F
3	13–14 Apr	13/1600	13/1900	14/0100	9	99 868	H, F
4	29 Apr	29/0000	29/0600	29/1200	12	293 510	H, T, W, L
5	4–5 May	4/2300	5/0500	5/1200	13	257 481	H, W
6	5–6 May	5/0400	5/1600	6/0700	27	177 215	W, T, L
7	5 May	5/1700	5/2000	5/2300	6	63 163	W, T, L
8	27–28 May	27/2200	28/0000	28/0400	6	121 907	H, W, L
9	28 May	28/0500	28/0800	28/1800	13	156 049	H, L, W
10	2 Jun	2/0300	2/0500	2/1000	7	70 622	H, W
11	9–10 Jun	9/1600	10/0700	10/1400	22	231 572	H, F, W
12	14 Jun	14/1200	14/1500	14/1800	6	96 161	H, L, F
13	15–16 Jun	15/1600	15/1900	16/0100	9	84 873	H, L, T
14	15–16 Jun	15/2300	16/0700	16/1800	19	351 442	H, W, L, F, T
15	23–24 Jun	23/2200	24/0600	24/1300	15	229 260	W, T, F, H
16	29–30 Jun	29/0200	30/0700	30/0700	29	207 246	W, H, L, T, F
17	1 Jul	1/0000	1/0600	1/1100	11	313 246	F, H, L, T
18	3 Jul	3/0400	3/0600	3/2200	18	151 900	T, H, W, F, L
19	6 Jul	6/1200	6/1800	6/2100	9	107 767	W, F, H, T
20	7 Jul	7/0400	7/0900	7/1400	10	165 263	T, F, W
21	8 Jul	8/0400	8/0700	8/1200	8	153 173	F, W, H, L, T
22	21–22 Jul	21/2300	22/0300	22/1000	11	146 776	H, T, W, F
23	23 Jul	23/0500	23/1400	23/1500	10	152 263	F
24	24 Jul	24/0200	24/1100	24/1400	12	193 912	H, F
25	26–27 Jul	26/2300	27/0400	27/1100	12	204 262	H, T, W
26	12 Aug	12/0400	12/1000	12/1600	12	261 893	F
27	14 Aug	14/0100	14/1400	14/1800	17	152 513	F, L
28	13–14 Sep	13/0600	13/1300	14/0000	18	171 030	H, W, T

rences were slightly less frequent in June–July 1993 than the climatological mean for June–July (18 compared with 20) and slightly larger (as indicated by the $-52°C$ cloud area) in 1993 than 1992. However, when taking into account all large, long-lived convective system occurrences in 1993, the frequency of occurrence cannot be downplayed so easily.

4. Analysis of environments associated with MCC and PECS initiation

a. Fixed-point composites

The most active 2-month period in March 1992–September 1993 was June–July 1993, when 24 PECSs and 18 MCCs were observed. The mean 500-mb geopotential height field for June–July 1993 contains a trough in the northwestern United States with a broad ridge extending over the remaining two-thirds of the nation (Fig. 8). Bell and Janowiak (1995) compared the mean 500-mb geopotential heights for June–July 1993 with mean June–July 500-mb geopotential heights defined from a base period of 1979–88. Their deviation plots reveal negative height anomalies as large as 60 m in the northwestern United States, and they suggest that the trough was part of a deep tropospheric baroclinic wave. According to baroclinic wave theory (Holton 1992), a divergent center is expected downwind of an upper-level trough as a result of the broad region of ascent associated with positive differential vorticity advection. Further, Bell and Janowiak (1995) noted that the right entrance region of a mean 200-mb jet streak coincided with the region of differential positive vorticity advection. The superposition of the direct thermal circulation of the jet streak (Murray and Daniels 1952; Chen and Kpaeyah 1993) and the divergence center associated with the continental scale baroclinic wave suggests the potential for anomalously strong synoptic-scale ascent over the Midwest. As we stated in the introduction, Augustine and Howard (1988) found that the large-scale circulation favorable for persistent MCC development was characterized by deep, phased synoptic-scale ascent. The results of our tabulation indicate that an upper-level circulation characterized by synoptic-scale ascent supports frequent PECS development also.

Our plots of deviation 500-mb geopotential height further support the notion that the upper-air circulation associated with MCC and PECS occurrences in June–July 1993 was characterized by synoptic-scale ascent, although the orientation of the upper-air features differed. Negative height anomalies in the northeastern and northwestern United States and a positive height anomaly over the central United States signify a higher-amplitude wave pattern relative to the mean 500-mb geopotential height for days in June–July 1993 when MCC occurrences were observed (Fig. 8a). In other words, our deviation 500-mb geopotential height composite is

TABLE 6. As in Table 2 except for PECS occurrences in 1993.

Case number	Date(s)	Initiation (Date/UTC)	Maximum	Termination	Duration (h)	Max. extent (km^2)	Significant Wx
1	24 Mar	24/0100	24/0400	24/1100	10	154 516	F
2	29–30 Mar	29/2000	30/0400	30/1200	16	221 053	H, W, L, T, F
3	30–31 Mar	30/1800	30/2000	31/0000	6	174 486	H, W, T, F
4	30–31 Mar	30/2100	31/0400	31/2200	25	211 169	H, W, L
5	3–4 Apr	3/2300	4/1000	4/1400	15	317 306	H, W, L
6	19 Apr	19/0100	19/1100	19/1500	14	203 333	H, W, L
7	1 May	1/0000	1/0400	1/1100	11	243 388	W, H
8	1 May	1/1900	1/2100	2/0100	6	104 633	W, H
9	2–3 May	2/0000	2/0500	3/0500	29	232 711	H, W, T
10	4 May	4/0700	4/0800	4/1500	8	163 078	No report
11	6 May	6/0000	6/0300	6/1400	14	269 960	W, T, L
12	15–16 May	15/2300	16/0500	16/0700	8	124 294	H
13	17–18 May	17/2300	18/0400	18/1200	13	363 143	W, H, T, F, L
14	18–19 May	18/1600	18/2300	19/0400	12	335 537	W, H, T, L, F
15	22–23 May	22/2300	23/0300	23/0900	10	132 719	T, H, W, F
16	30 May	30/0100	30/0600	30/0900	8	103 964	H, W, F
17	2–3 Jun	2/2200	3/0400	3/1700	19	169 099	T, H, W
18	4–5 Jun	4/0500	4/1500	5/0000	19	329 599	H, W, T, L, F
19	5 Jun	5/0000	5/0400	5/1000	10	148 262	W, T, H
20	8 Jun	8/0000	8/0200	8/1200	12	350 217	T, W, H, L
21	8–9 Jun	8/1300	8/2000	9/0700	18	159 202	H, W, F, T
22	13 Jun	13/0600	13/1000	13/1700	11	227 482	H, W
23	14 Jun	14/0000	14/0300	14/1000	10	208 996	T, W, F, L
24	14–15 Jun	14/1800	15/0000	15/0800	14	161 656	W, H, F, L
25	19 Jun	19/0100	19/0300	19/0800	7	113 891	H, F, W
26	23 Jun	23/0000	23/0300	23/2300	23	150 179	W, H, T
27	25 Jun	25/0000	25/0200	25/1500	15	222 533	W, H, F
28	2 Jul	2/0200	2/0600	2/1000	8	208 929	F, H, T, W
29	3 Jul	3/1300	3/1400	3/2000	7	93 506	F, L, T
30	7 Jul	7/0000	7/0400	7/0800	8	226 105	H, L, W, F
31	9 Jul	9/0200	9/0500	9/0800	6	223 706	H, W, T, F
32	13 Jul	13/0100	13/1000	13/1400	13	126 866	F, L
33	21 Jul	21/0100	21/0700	21/1200	11	138 214	T, W, H, F
34	23 Jul	23/0500	23/0900	23/1100	6	114 976	F
35	24 Jul	24/0500	24/0800	24/1200	7	284 222	F
36	26–27 Jul	26/2000	27/0100	27/0400	8	208 661	W, F, L
37	6 Aug	6/0000	6/0100	6/0700	7	117 877	W, L, H, T
38	9 Aug	9/0300	9/0900	9/2100	18	110 418	T, W
39	10 Aug	10/0100	10/0800	10/1500	14	149 580	H, W, F
40	11 Aug	11/0100	11/0300	11/1500	14	122 874	H, W
41	12 Aug	12/2300	13/0300	12/1200	13	256 683	F
42	13 Sep	13/0900	13/1200	13/1700	8	118 422	L, W, F, T
43	13–14 Sep	13/2100	13/2200	14/1200	15	174 380	F, T, W
44	14 Sep	14/0100	14/0500	14/1900	18	227 487	W, T, F

similar to the 500-mb geopotential height composite in Bell and Janowiak (1995), except that the negative anomaly over the northwestern United States in our plots implies a larger deviation from the 1979–88 mean. Augustine and Howard (1991) diagnosed a high-amplitude wave pattern in the 500-mb geopotential height for periods of active MCC development in 1986 and 1987 that was dominated by ridging in the central United States, in contrast with the dominant troughing along the United States west coast in June–July 1993. PECS occurrences in June–July 1993 favored initiation downwind of a trough within a continental-scale wave as the trough exited the intermountain region. This is indicated by a broad 500-mb geopotential height minimum east of the background state trough (Fig. 8b).

The southern edge of the 200-mb jet stream was situated over the Midwest on days when MCC occurrences were observed in June–July 1993 (Fig. 9a). Unlike the mean June–July 1993 200-mb wind, the upper-level circulation does not contain a jet streak. Instead, assuming the thermal wind relation, the zonal jet stream implies a zonal low-level thermal boundary. This is consistent with the large-scale composites performed by Augustine and Howard (1991), who observed that low-level thermal forcing and convective instability when phased vertically with a mid- to upper-level anticyclone was the most favorable pattern for MCC development. However, a 200-mb jet streak is resolved in the 200-mb deviation wind for the PECS occurrences in June–July 1993 (Fig. 9b), suggesting that upper-level jet streak circulations directly influence PECS initiation more frequently than MCC initiation.

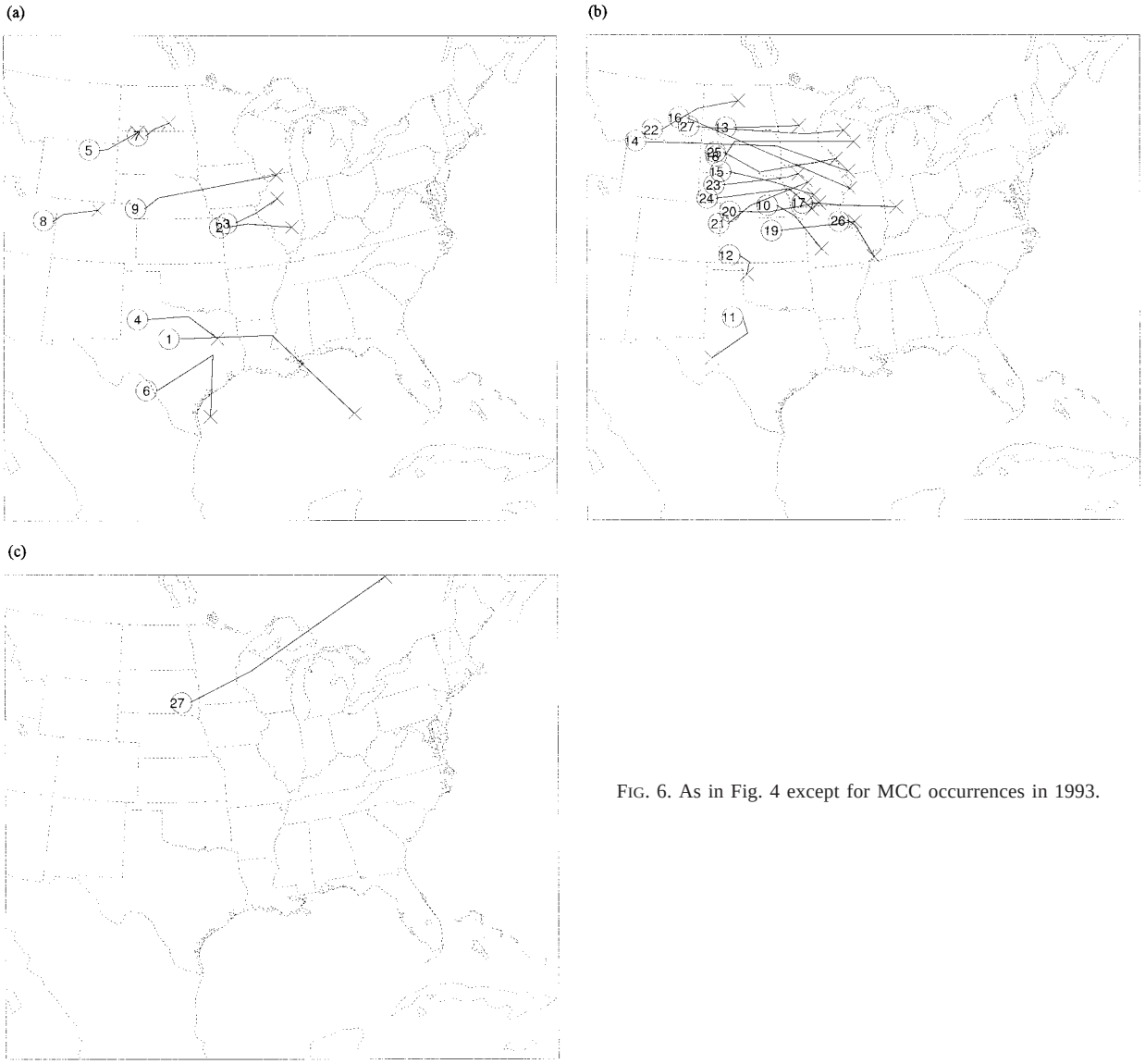

FIG. 6. As in Fig. 4 except for MCC occurrences in 1993.

b. Storm-relative composites

1) UPPER-LEVEL FEATURES

Both MCC-relative and PECS-relative composites of 200-mb relative vorticity (Fig. 10) reveal that a continental-scale wave dominates the upper-level environment prior to initiation of either type of convective system. Consistent with the fixed-point composites, the continental-scale wave in the PECS-relative composite is situated east of the continental-scale wave in the MCC-relative composite. The continental-scale wave in the PECS-relative composite is also a deep tropospheric wave, whose westward tilt with height (Fig. 10b) resembles the westward tilt with height expected for a *developing* baroclinic wave (Holton 1992). In contrast, the MCC-relative composite of 700-mb relative vorticity indicates the presence of a short-wavelength disturbance passing the trough axis and impinging on the composite MCC position of initiation from the southwest.

A short wavelength feature was resolved by Maddox (1983) upstream of his composite MCC position of initiation, but a storm-relative composite by Cotton et al. (1989) did not resolve this feature. The composite by Cotton et al. (1989) contained more samples, but the samples were limited to MCC occurrences during the summer. Therefore, their composite contained less variability among samples than both Maddox (1983) and our composite. While the results of Cotton et al. (1989) are less likely to contain nonphysical short-wavelength features introduced by including a seasonal trend in the composite, their results may not reflect the variety of atmospheric circulations that support MCC occurrences.

In order to examine the influence of sample selection in our composite, we constructed two MCC-relative

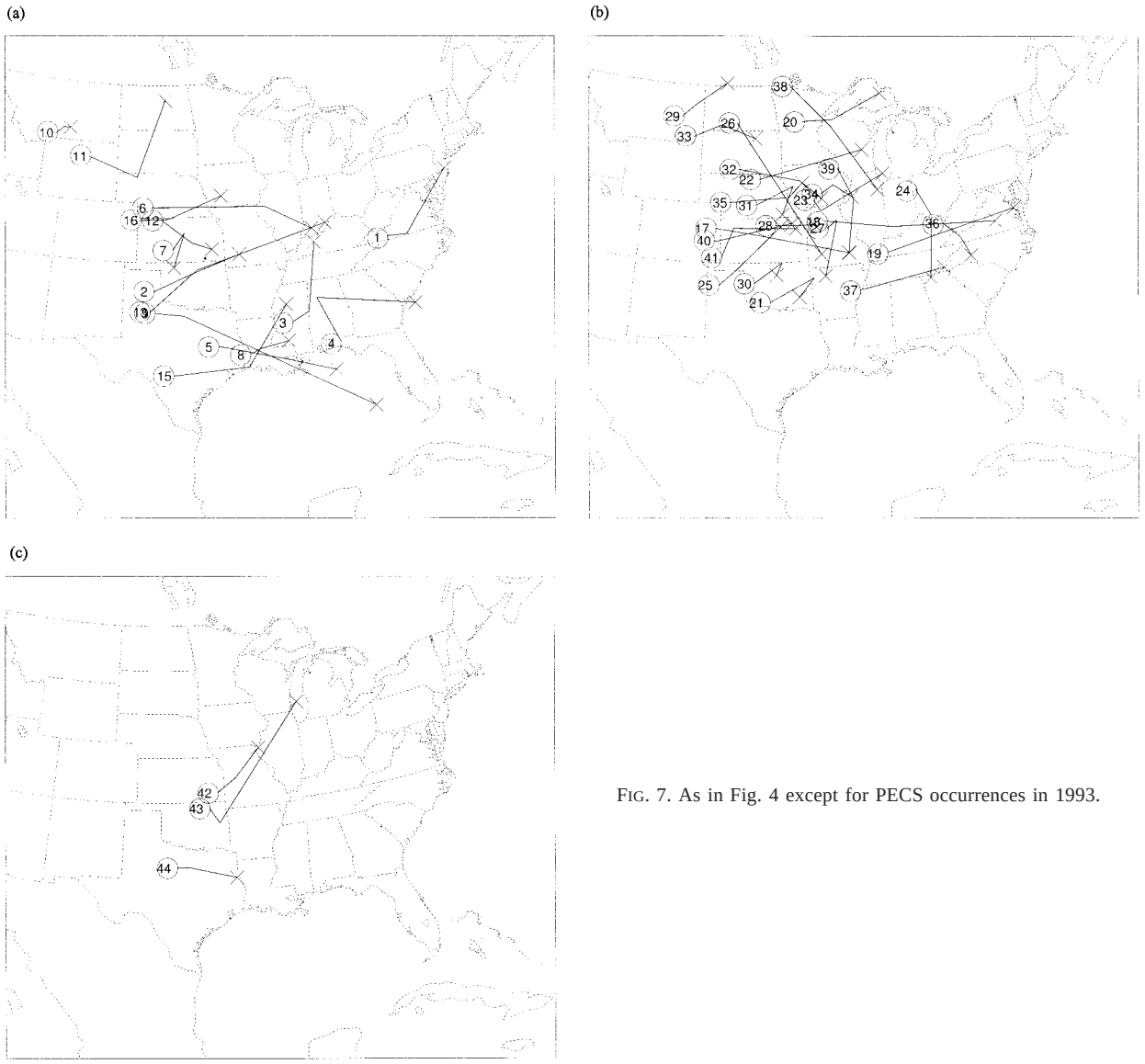

FIG. 7. As in Fig. 4 except for PECS occurrences in 1993.

composites for 200- and 700-mb relative vorticity and 200-mb wind (not shown here). One composite contained only MCC occurrences during the summer, while the other composite contained only MCC occurrences during spring and fall. Both composites of 200-mb relative vorticity exhibited the upper-level continental-scale wave previously discussed, but the short-wavelength feature produced a much stronger signal in the spring–fall MCC composite. These results suggest that the discrepancy between Cotton et al. (1989) and Maddox (1983) may result simply from the differences in the sample selection.

2) ROLE OF SHORT-WAVELENGTH DISTURBANCES

The discussion by Augustine and Howard (1991) summarized two main schools of thought on the influence of short-wavelength disturbances in the development of MCC occurrences. First, Velasco and Fritsch (1987) proposed that the ascending motion associated with short-wavelength disturbances directly enhances MCC development as suggested by the composites presented in Maddox (1983). The second school of thought proposed that short-wavelength disturbances promote low-level cold-air advection enhancing low-level frontogenetic circulations. The cold-air advection mechanism does not require that short-wavelength disturbances be in close proximity to the MCC occurrence in either space or time to influence MCC development. The latter theory is more plausible when MCC occurrences develop in rapid succession (Schwartz et al. 1990) and establishes consistency between the results of Maddox (1983) and Cotton et al. (1989).

Our composites also support the notion that a short-

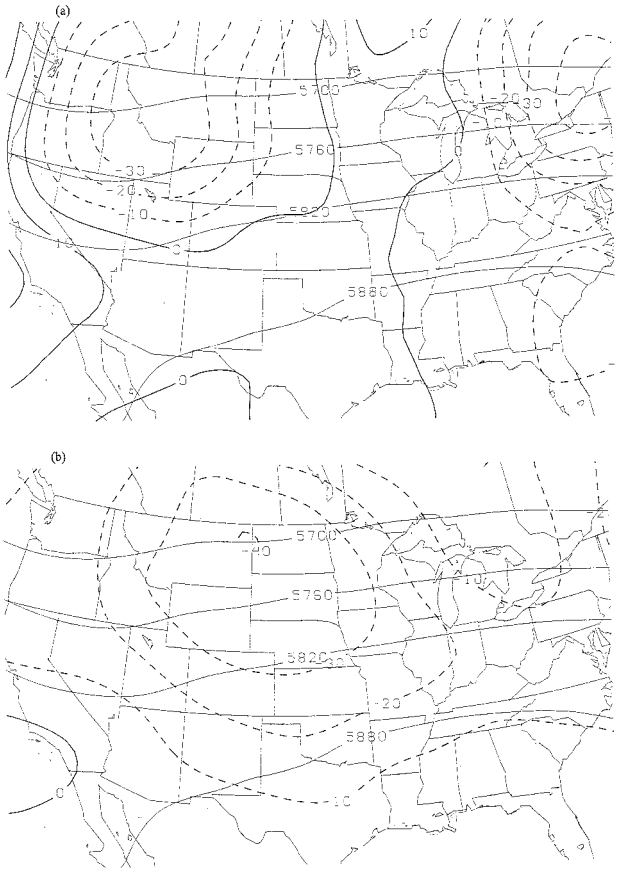

FIG. 8. Mean June–July 1993 500-mb geopotential height (m, thin lines) and deviation (thick lines) for days in June–July 1993, when (a) MCC occurrences and (b) PECS occurrences were observed.

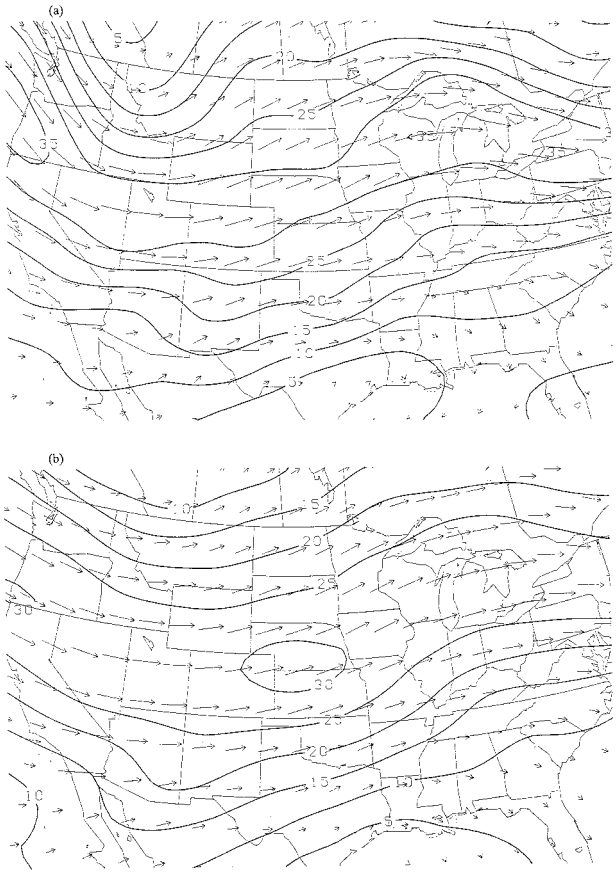

FIG. 9. The 200-mb composite wind vectors and speed (m s^{-1}) for days in June–July 1993, when (a) MCC occurrences and (b) PECS occurrences were observed.

wavelength disturbance frequently influences the development of MCCs. Upper-level divergence (Fig. 11a) extends from near the position of the short-wavelength disturbance through the inflection point of the continental-scale baroclinic wave with a maximum directly east of the short-wavelength feature. The short-wavelength feature enhances and expands the region of upper-level divergence within the continental-scale wave. In this way, mid- to upper-level ascent associated with the short-wavelength disturbance enhances MCC initiation directly, similar to the role proposed by Velasco and Fritsch (1987). However, short-wavelength disturbances may indirectly influence MCC development as the short-wavelength disturbance approaches the axis of the continental-scale trough. Vorticity advection ahead of the short-wavelength disturbance intensifies the cyclone and increases the amplitude of the continental-scale wave. (We infer this from the definition of geostrophic relative vorticity in isobaric coordinates, which shows that local maxima of geostrophic relative vorticity are proportional to local minima of geopotential height. Therefore, positive geostrophic relative vorticity advection generally corresponds to the movement of geopotential height minima.) Increasing the amplitude of the continental-scale wave also enhances the upper-level divergence associated with the continental-scale wave. As previously discussed, high-amplitude continental-scale waves are often observed with frequent MCC development.

3) UPPER-LEVEL DYNAMIC CIRCULATION

Consistent with previous MCC studies, we find that a deep tropospheric dynamic circulation is important to the development of MCCs and appears to be important to PECSs as well (Fig. 11b). The stronger upper-level divergence maximum in the PECS-relative 200-mb divergence (Fig. 11) suggests stronger upper-level dynamics are associated with the systems that support PECS development. Additional upper-level support is provided by the cross-jet circulation at the right entrance region of the 200-mb jet streak in both MCC-relative and PECS-relative 200-mb wind composites (Fig. 12). Recall that the fixed-point MCC composite did not resolve a 200-mb jet streak. This discrepancy may result from the smoothing that occurs with the fixed-point method, or it may indicate that a jet streak was not observed very often within the sample used for the fixed-point

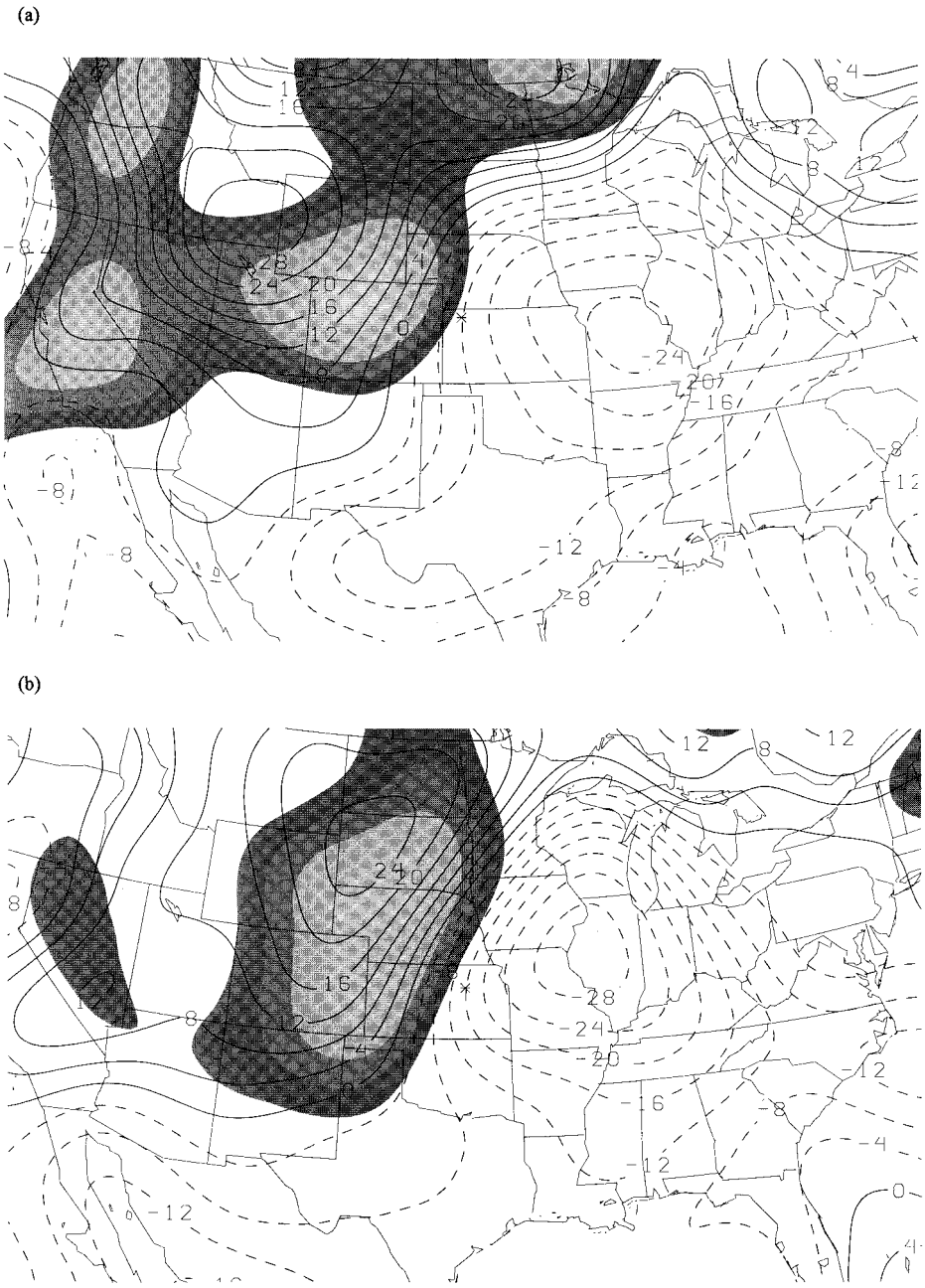

FIG. 10. The 200-mb relative vorticity (1×10^{-6} s^{-1}, contoured) and 700-mb relative vorticity (1×10^{-6} s^{-1}, shaded with interval of 2 starting with 2) for (a) MCC-relative and (b) PECS-relative composites. Asterisk denotes position of initiation for the composite convective system.

composite (containing only MCC occurrences in June–July 1993). The latter explanation is supported by the fact that a stronger and more compact jet streak was resolved in our spring–fall MCC-relative composite when compared to our summer MCC-relative composite of 200-mb wind.

We provide a measure of the synoptic-scale ascent with composites of **Q**-vector divergence at 300 and 700

→

FIG. 11. The 200-mb divergence (1×10^{-6} s^{-1}, contoured) and 850-mb convergence (1×10^{-6} s^{-1}, shaded with interval of -2 starting with -4) for (a) MCC-relative and (b) PECS-relative composites.

(a)

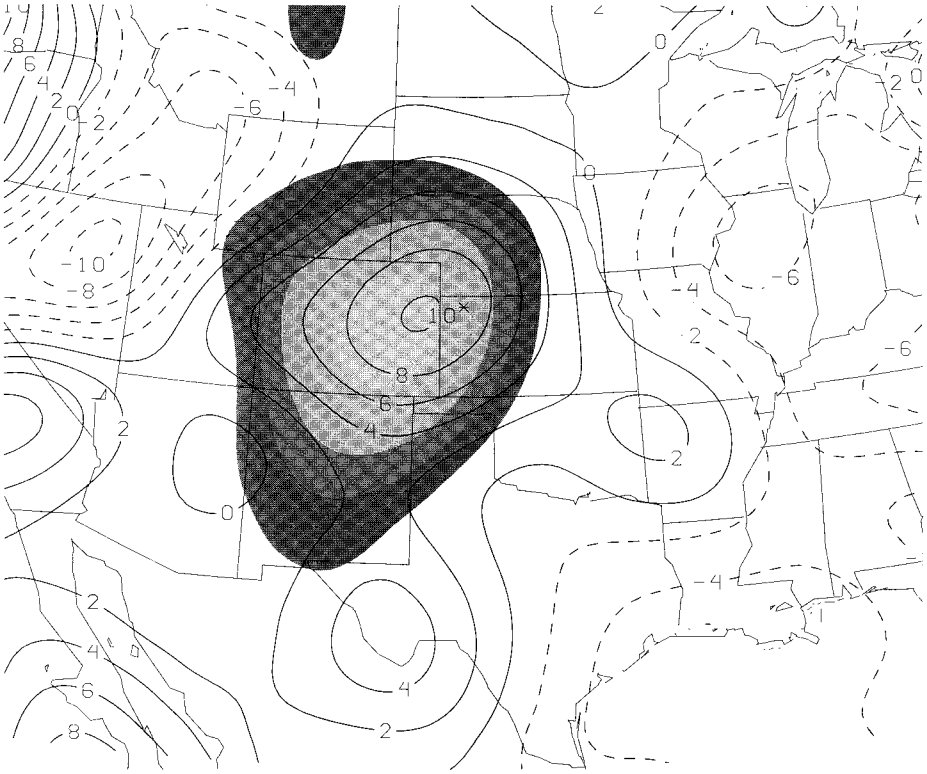

(b)

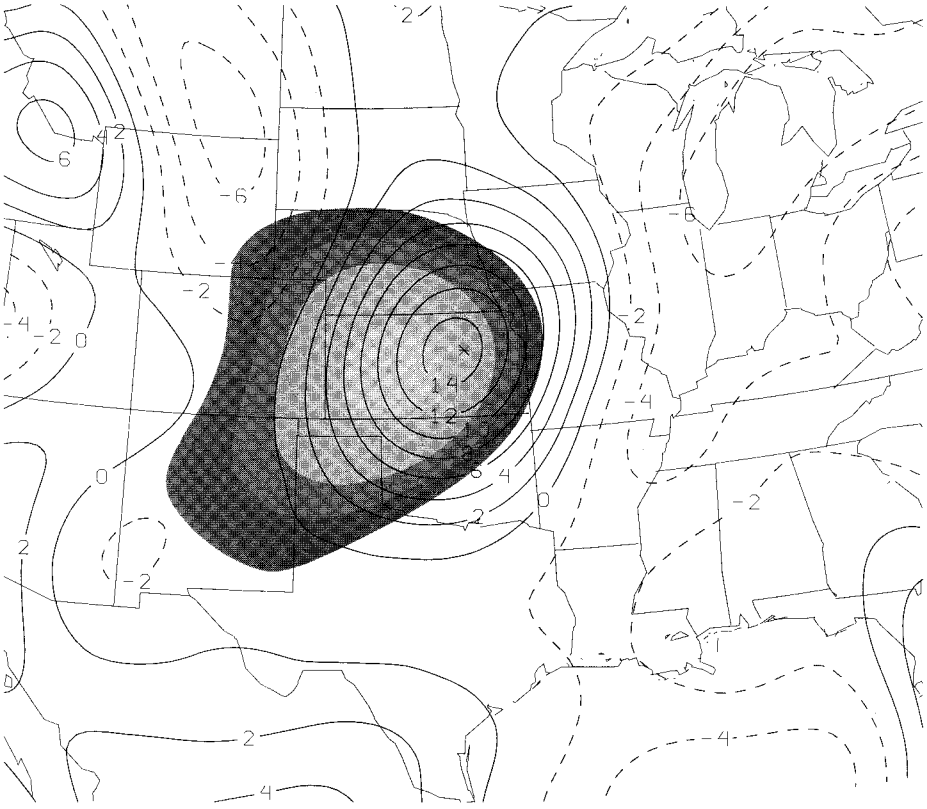

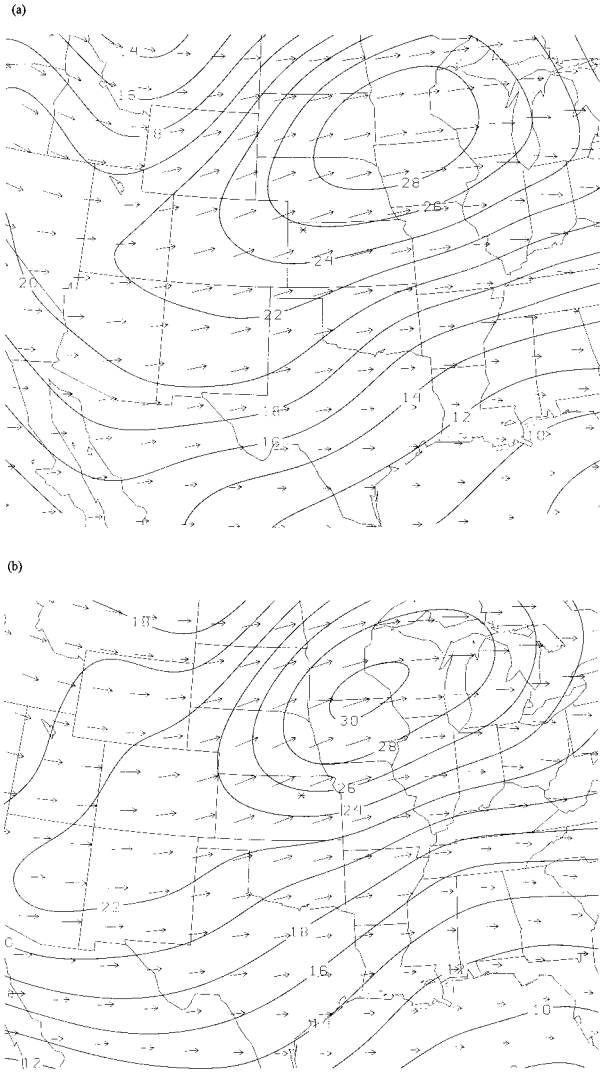

FIG. 12. (a) MCC-relative and (b) PECS-relative composites of 200-mb wind vector and wind speed (m s^{-1}).

mb (Fig. 13). A region of deep synoptic-scale ascent that tilts slightly north and west with height is associated with the deep tropospheric dynamic circulation in both MCC and PECS composites. Deep synoptic-scale ascent has been diagnosed near the time of initiation of MCC occurrences by Maddox (1983) and Cotton et al. (1989) and is consistent with the fixed-point composites we presented earlier. However, in the PECS composite, the synoptic-scale ascent is somewhat stronger, supporting our earlier assertion that, in general, dynamic forcing is stronger with PECS occurrences than MCC occurrences.

4) LOW-LEVEL FEATURES

MCCs often initiate near the intersection of an LLJ (low-level jet) and a zonally oriented quasi-stationary front or warm front (Augustine and Howard 1991; Augustine and Caracena 1994). Many circulations that produce local maxima in meso- to synoptic-scale ascent and support convective initiation are induced by this intersection. A few examples mentioned in the literature are frontogenetic circulations (Augustine and Caracena 1994), frontal overrunning (isentropic lift), and convergence (Cotton et al. 1989). In 1993, convergence associated with the LLJ played an important role in the extremely active period in late June and early July. Arritt et al. (1997) derived a composite of the 1200 UTC 850-mb ageostrophic wind component for days when a strong LLJ (>20 m s^{-1}) was observed over the central United States (29–30 June, 3–9 July, and 14 July 1993). Convergence is evident in their composite over the same region (near 40°N) where 11 large, long-lived convective systems were observed during the period extending 29 June–10 July.

In addition to inducing ascent, the LLJ supplies moisture to the MCC by advecting higher-θ_e air into the region of initiation (Cotton et al. 1989). Figure 14 portrays this scenario for the MCC-relative composite and many similar features for the PECS-relative composite. The LLJ is observed south of the composite MCC and composite PECS position of initiation. In both composites, the LLJ advects moisture from the Gulf of Mexico into the region of initation and eastward. The eastward extension of moisture advection highlights the importance of low-level moisture transport to the sustenance of both types of large, long-lived convective systems. Drying is observed southwest of the initation position in both composites. The presence of westerly flow and drying along, and west of, a north–south-oriented confluent zone that is better defined in the PECS composite indicates that drying in the PECS composite is associated with an airmass boundary such as a dryline or a cold front. Drying ahead of the confluence zone in the MCC composites indicates moisture transport from a region southwest of the initiation position to the region of initiation and eastward. In our composites, PECS occurrences tended to tap a moisture source to the southeast or south of the region of initation, whereas MCC occurrences tapped moisture south or southwest of the region of initiation. Moisture advection in the MCC composite is bounded to the north by a region of confluence that probably represents a warm or stationary front. This boundary is more defined in the MCC composite and confines moisture transport over the region.

This east–west boundary may also limit the areal extent of convective initiation. The boundary is situated within the region of the upper-level synoptic-scale ascent (Figs. 13a and 14a). Because conditional instability tends to be less likely on the cold side of low-level thermal boundaries, the boundary limits the northward extent over which upper-level ascent aids convection. In comparison, the north–south boundary in the PECS-relative composite does not limit the northward or southward extent over which upper-level ascent may aid convection.

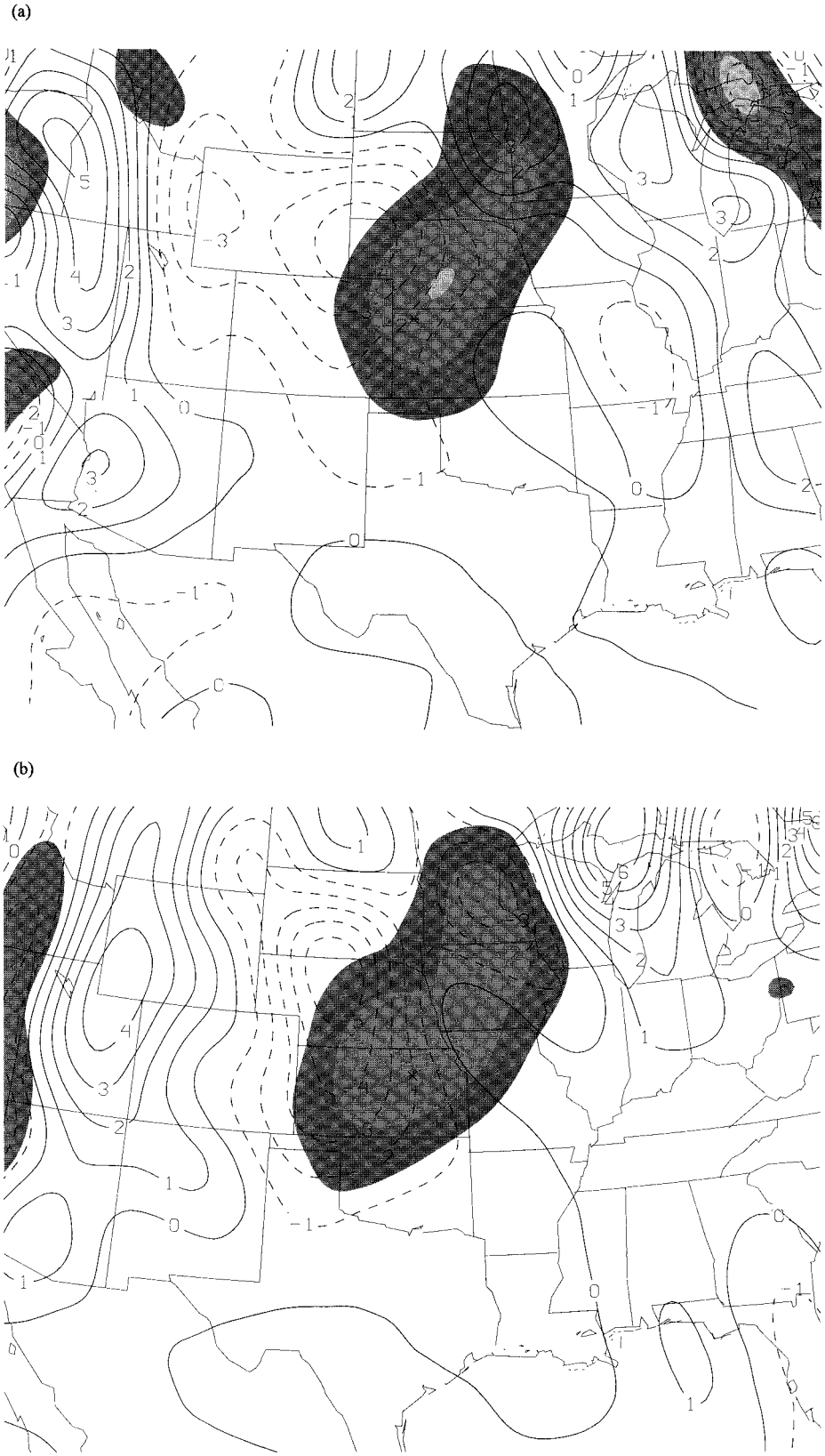

FIG. 13. The 300-mb **Q**-vector divergence (1×10^{-16} s^{-3} mb^{-1}, contoured) and 700-mb **Q**-vector divergence (1×10^{-16} s^{-3} mb^{-1}, shaded with interval of -1 starting with -1) for (a) MCC-relative and (b) PECS-relative composites.

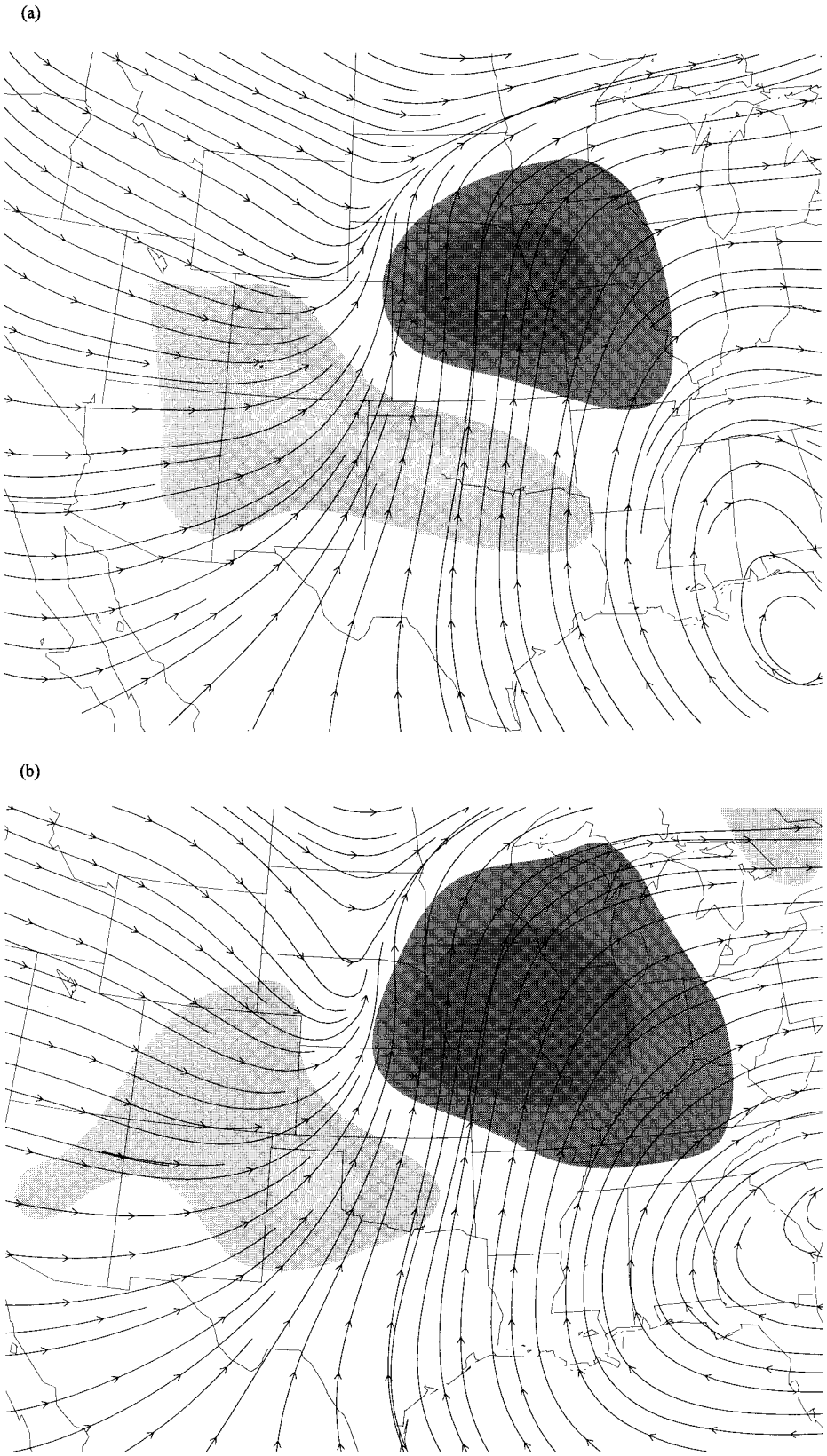

FIG. 14. Streamline analysis derived from the recononstructed 850-mb wind and 850-mb moisture advection [1×10^{-2} g kg^{-1} h^{-1}, shaded with intervals of ≤ -6 (lightest), -6 to -3, -3 to 3 (no shading), 3 to 6, ≥ 6 (darkest)] for (a) MCC-relative and (b) PECS-relative composites.

Convection may also be hindered by the presence of low-level inversions. Carlson and Farrell (1983) introduced a lid-strength term using the difference between the maximum saturated wet-bulb potential temperature within the inversion and the surface wet-bulb potential temperature (term B of the lid-strength index). Because our dataset consists solely of mandatory-level data, we used the 700-mb saturated wet-bulb potential temperature in place of the maximum saturated wet-bulb potential temperature within the inversion and replaced the surface wet-bulb potential temperature with the 850-mb wet-bulb potential temperature. While our substitutions prohibit a direct comparison with lid-strength threshold values for surface-based convection (Farrell and Carlson 1989), the general result that convective inhibition increases with the lid-strength term is retained.

The initiation position in the MCC composite lies immediately eastward and northward of a region of increasing lid strength (Fig. 15a), resembling the underrunning process associated with some severe convective storms (Farrell and Carlson 1989). This region of increasing lid strength hinders convection and limits the southward extent of the convective system. In contrast, a local minimum and weaker gradient of the lid strength is observed near the initiation position in the PECS composite. This implies that convection is not as effectively inhibited, especially if the meridionally oriented confluence is interpreted as a thermal boundary.

In both the MCC and PECS composites, the LLJ appears to be induced in part by the upper-level dynamic forcing (Uccellini and Johnson 1979; Uccellini 1980; Arritt et al. 1997). Figure 15 reveals a southerly component in the deviation wind field that is in close proximity to the vertically phased divergence and convergence in Fig. 11. In a composite of the springtime LLJ (Chen and Kpaeyah 1993), the composite LLJ was positioned within the low-level branch of the divergent circulation associated with a developing continental-scale baroclinic wave. The exit region of an upper-level jet streak is positioned near the upper-level divergent center in their composite so that the direct cross-jet circulation enhances a portion of the upper-level divergence and, subsequently, accelerates a portion of the low-level branch of the divergent circulation producing a local wind maximum. This LLJ mechanism is consistent with the superposition of a divergent center associated with the continental-scale wave with an upper-level jet streak in both MCC-relative and PECS-relative composites. By positioning and enhancing the low-level moisture transport in this manner, the upper-level dynamic forcing can indirectly influence the position and development of MCC and PECS occurrences.

Notice that the gradient of the wind speed along the upper-lever jet streak axis is slightly less in the MCC-relative composite than in the PECS-relative composite. This means that either upper-level jet streaks are not as common, or they are not as strong. Despite this observation, the southerly component in the MCC deviation streamline composite extends a greater distance south of the initiation position than in the PECS composite. Therefore, acceleration of the low-level branch of the divergent circulation in the MCC-relative composite may reflect additional physical processes. Stull (1988) describes many boundary layer processes that induce low-level wind maxima. For example, differential heating over sloped terrain induces a surface pressure gradient and accelerates the low-level flow. Consistent with this boundary layer mechanism, the LLJ is positioned over sloped terrain within a moisture gradient (Fig. 14a). Or, the LLJ may be related to other synoptic-scale circulations such as the westward extension of the Bermuda high, which is often observed with MCC occurrences (Augustine and Howard 1991). A more complete discussion of boundary layer and synoptic-scale influences on the LLJ is provided in Augustine and Caracena (1994) and Stensrud (1996).

5. Summary

We have cataloged 27 MCC occurrences and 77 PECS occurrences in 1992, and 28 MCC occurrences and 44 PECS occurrences in 1993. Both MCC and PECS occurrences tended to be nocturnal and were observed most often during the summer. The average duration and maximum areal coverage of the -52°C cloud shield of MCC and PECS occurrences were comparable. The spatial distribution of PECS occurrences displayed a mean seasonal shift similar to the climatological distribution of MCC occurrences but displayed greater variability and a tendency for PECS to initiate and develop farther east than MCCs. PECS occurrences displayed more variability in time of initiation, position of initiation, size, and duration than MCC occurrences. Spatial coherence in the distribution of both MCC and PECS occurrences, *and* the frequency of PECS occurrences, contributed to the extreme wet period extending from July 1992 to August 1993 that culminated in the regional flooding in the central plains.

While the cloud-shield shape differs, both convective-system types initiated in environments that are characterized by deep, synoptic-scale ascent and low-level moisture transport from a southerly LLJ associated with continental-scale baroclinic waves. PECS occurrences initiated more often when vigorous waves exited the intermountain region, whereas MCC occurrences initiated more often within a high-amplitude wave pattern with a trough positioned over the northwestern United States and a ridge positioned over the central Great Plains.

Provided this upper-level support, an important element that organizes local convection into different types of convective systems (based on the shape of the cloud shield) appears to be the orientation of low-level thermal features. In the MCC-relative composite, convection is focused to a particular region by low-level inversions south and west of the initiation position and an east–

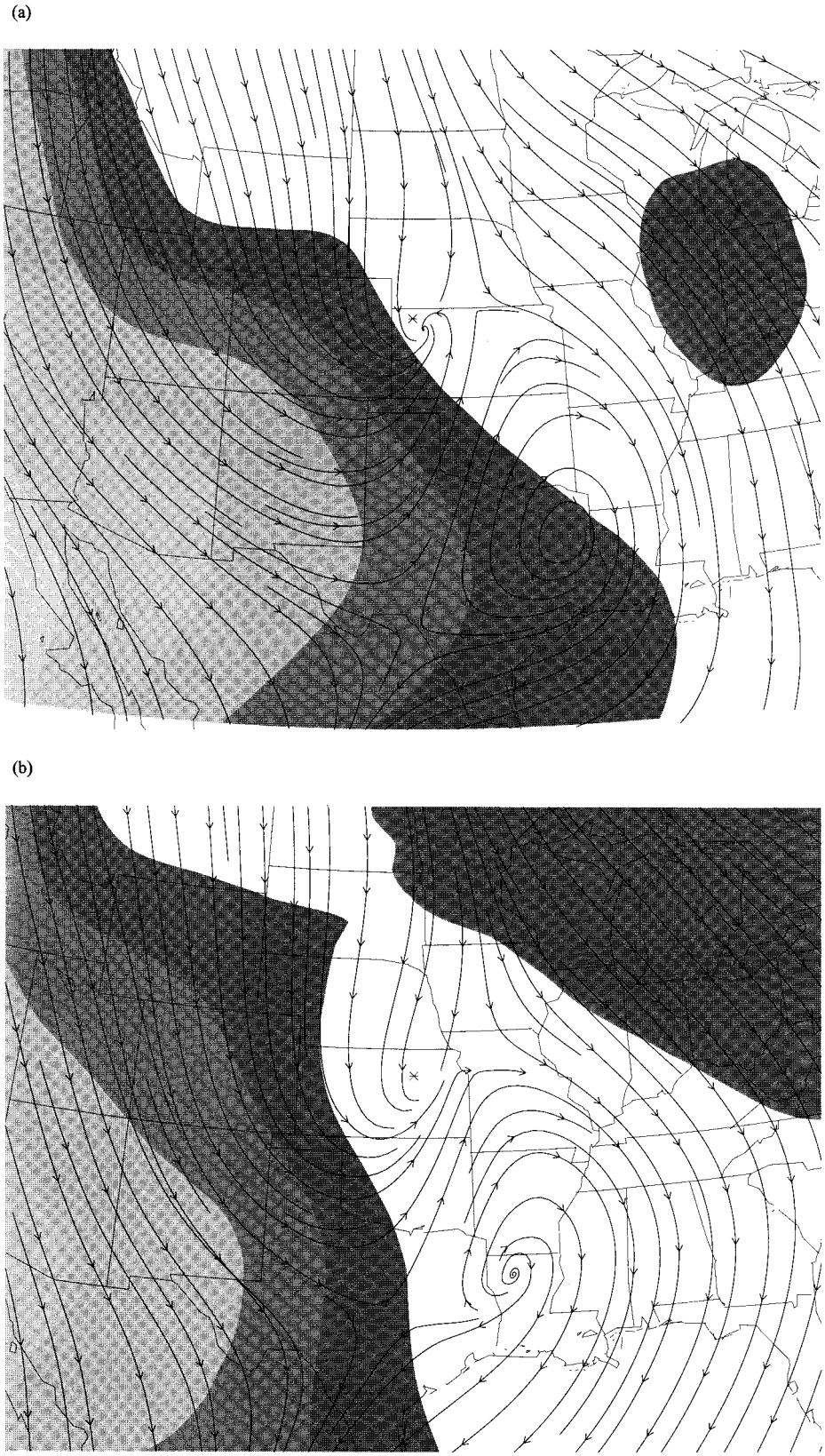

FIG. 15. Streamline analysis derived from the 850-mb deviation wind and lid-strength term (°C, shaded with interval of 1 starting with 1) for (a) MCC-relative and (b) PECS-relative composites.

west boundary north of the initiation position. In the PECS composite, the areal coverage of convection is not as effectively hindered by low-level inversions and may be aided by a north–south thermal boundary.

Acknowledgments. This research was supported by NSF Grants ATM-9627890 and ATM-9616728. We are grateful to John Augustine for providing the automated satellite classification software and assisting with its implementation. We also thank Dr. Arlene Laing for useful discussions on MCCs. Reviews by Dr. Laing and two anonymous reviewers considerably aided the presentation and substance of this paper. This is Journal Paper J-17681 of the Iowa Agriculture and Home Economics Experiment Station, Ames, Iowa, Project No. 3245, and supported by Hatch Act and State of Iowa funds.

REFERENCES

Achtemeier, G. L., 1989: Modification of a successive corrections objective analysis for improved derivative calculations. *Mon. Wea. Rev.,* **117,** 78–86.

Arritt, R. W., T. D. Rink, M. Segal, D. P. Todey, C. A. Clark, M. J. Mitchell, and K. M. Labas, 1997: The Great Plains low-level jet during the warm season of 1993. *Mon. Wea. Rev.,* **125,** 2176–2192.

Augustine, J. A., 1985: An automated method for the documentation of cloud-top characteristics of mesoscale convective systems. NOAA Tech. Memo. ERL ESG-10, Dept. of Commerce, Boulder, CO, 121 pp. [Available from NOAA/FLS, 325 Broadway, Boulder, CO 80303.]

——, and K. W. Howard, 1988: Mesoscale convective complexes over the United States during 1985. *Mon. Wea. Rev.,* **116,** 685–701.

——, and ——, 1991: Mesoscale convective complexes over the United States during 1986 and 1987. *Mon. Wea. Rev.,* **119,** 1575–1589.

——, and F. Caracena, 1994: Lower-tropospheric precursors to nocturnal MCS development over the central United States. *Wea. Forecasting,* **9,** 115–135.

Barnes, S. L., 1994: Applications of the Barnes objective analysis scheme. Part III: Tuning for minimum error. *J. Atmos. Oceanic Technol.,* **11,** 1459–1479.

Bartels, D. L., J. M. Skradski, and R. D. Menard, 1984: Mesoscale convective systems: A satellite-data-based climatology. NOAA Tech. Memo. ERL ESG 8, Dept. of Commerce, Boulder, CO, 63 pp. [NTIS PB-85-187904.]

Bell, G. D., and J. E. Janowiak, 1995: Atmospheric circulation associated with the Midwest floods of 1993. *Bull. Amer. Meteor. Soc.,* **76,** 681–695.

Carlson, T. N., and R. J. Farrell, 1983: The lid strength index as an aid in predicting severe local storms. *Natl. Wea. Dig.,* **8,** 769–774.

Chen, T.-C., and J. A. Kpaeyah, 1993: The synoptic-scale environment associated with the low-level jet of the Great Plains. *Mon. Wea. Rev.,* **121,** 416–420.

Cotton, W. R., M.-S. Lin, R. L. McAnnelly, and C. J. Tremback, 1989: A composite model of mesoscale convective complexes. *Mon. Wea. Rev.,* **117,** 765–783.

Farrell, R. J., and T. N. Carlson, 1989: Evidence for the role of the lid and underrunning in an outbreak of tornadic thunderstorms. *Mon. Wea. Rev.,* **117,** 857–871.

Fritsch, J. M., and R. A. Maddox, 1981: Convectively driven mesoscale pressure systems aloft. Part I: Observations. *J. Climate Appl. Meteor.,* **20,** 9–19.

——, R. J. Kane, and C. R. Chelius, 1986: The contribution of mesoscale convective weather systems to the warm-season precipitation of the United States. *J. Climate Appl. Meteor.,* **25,** 1333–1345.

Holton, J. R., 1992: *An Introduction to Dynamic Meteorology.* Academic Press, 511 pp.

Hoskins, B. J., I. Draghici, and H. C. Davies, 1978: A new look at the ω-equation. *Quart. J. Roy. Meteor. Soc.,* **104,** 3–38.

Kalnay E., M. Kanamitsu, and W. E. Baker, 1990: Global numerical weather prediction at the National Meteorological Center. *Bull. Amer. Meteor. Soc.,* **71,** 1410–1428.

Kunkel, K. E., S. A. Changnon, and J. R. Angel, 1994: Climatic aspects of the 1993 upper Mississippi River basin flood. *Bull. Amer. Meteor. Soc.,* **75,** 811–822.

Laing, A. G., and J. M. Fritsch, 1997: The global population of mesoscale convective complexes. *Quart. J. Roy. Meteor. Soc.,* **123,** 389–405.

Maddox, R. A., 1980: Mesoscale convective complexes. *Bull. Amer. Meteor. Soc.,* **61,** 1374–1387.

——, 1983: Large-scale meteorological conditions associated with midlatitude, mesoscale convective complexes. *Mon. Wea. Rev.,* **111,** 1475–1493.

——, D. M. Rodgers, and K. W. Howard, 1982: Mesoscale convective complexes over the United States during 1981—Annual summary. *Mon. Wea. Rev.,* **110,** 1501–1514.

Menard, R. D., and J. M. Fritsch, 1989: A mesoscale convective complex-generated inertially stable warm core vortex. *Mon. Wea. Rev.,* **117,** 1237–1259.

Murray, R., and S. M. Daniels, 1953: Transverse flow at entrance and exit to jet streams. *Quart. J. Roy. Meteor. Soc.,* **79,** 236–241.

Rodgers, D. M., K. W. Howard, and E. C. Johnston, 1983: Mesoscale convective complexes over the United States during 1982. *Mon. Wea. Rev.,* **111,** 2363–2369.

——, M. J. Magnano, and J. H. Arns, 1985: Mesoscale convective complexes over the United States during 1983. *Mon. Wea. Rev.,* **113,** 888–901.

Schwartz, B. E., C. F. Chappell, W. E. Togstad, and X.-P. Zhong, 1990: The Minneapolis flash flood: Meteorological analysis and operational response. *Wea. Forecasting,* **5,** 3–21.

Stensrud, D. J., 1996: Importance of low-level jets to climate: A review. *J. Climate,* **9,** 1698–1711.

Stull, R. B., 1988: *An Introduction to Boundary Layer Meteorology.* Kluwer Academic, 660 pp.

Uccellini, L. W., 1980: On the role of upper tropospheric jet streaks and leeside cyclogenesis in the development of low-level jets in the Great Plains. *Mon. Wea. Rev.,* **108,** 1689–1696.

——, and D. R. Johnson, 1979: The coupling of upper and lower tropospheric jet streaks and implications for the development of severe convective storms. *Mon. Wea. Rev.,* **107,** 682–703.

Velasco, I., and J. M. Fritsch, 1987: Mesoscale convective complexes in the Americas. *J. Geophys. Res.,* **92,** 9591–9613.

Zhang, D.-L., and J. M. Fritsch, 1987: Numerical simulation of the meso-β scale structure and evolution of the 1977 Johnstown flood. Part II: Inertially stable warm-core vortex and the mesoscale convective complex. *J. Atmos. Sci.,* **44,** 2593–2611.